

# Impact of large scale flows on turbulent transport

Y Sarazin<sup>1</sup>, V Grandgirard<sup>1</sup>, G Dif-Pradalier<sup>1</sup>, E Fleurence<sup>1</sup>, X Garbet<sup>1</sup>,  
Ph Ghendrih<sup>1</sup>, P Bertrand<sup>2</sup>, N Besse<sup>2</sup>, N Crouseilles<sup>3</sup>, E Sonnendrücker<sup>3</sup>,  
G Latu<sup>4</sup> and E Violard<sup>4</sup>

<sup>1</sup> Association Euratom-CEA, CEA/DSM/DRFC centre de Cadarache,  
13108 St-Paul-Lez-Durance, France

<sup>2</sup> LPMIA-Université Henri Poincaré Nancy I, Boulevard des Aiguillettes BP239,  
54506 Vandœuvre-lès-Nancy, France

<sup>3</sup> IRMA, UMR 7501 CNRS/Université Louis Pasteur, 7 rue René Descartes, 67084 Strasbourg,  
France

<sup>4</sup> LSIIIT, UMR 7005 CNRS/Université Louis Pasteur, Bd Sébastien Brant BP10413,  
67412 Illkirch, France

Received 23 June 2006

Published 10 November 2006

Online at [stacks.iop.org/PFCF/48/B179](http://stacks.iop.org/PFCF/48/B179)

## Abstract

The impact of large scale flows on turbulent transport in magnetized plasmas is explored by means of various kinetic models. Zonal flows are found to lead to a non-linear upshift of turbulent transport in a 3D kinetic model for interchange turbulence. Such a transition is absent from fluid simulations, performed with the same numerical tool, which also predict a much larger transport. The discrepancy cannot be explained by zonal flows only, despite they being overdamped in fluids. Indeed, some difference remains, although reduced, when they are artificially suppressed. Zonal flows are also reported to trigger transport barriers in a 4D drift-kinetic model for slab ion temperature gradient (ITG) turbulence. The density gradient acts as a source drive for zonal flows, while their curvature back stabilizes the turbulence. Finally, 5D simulations of toroidal ITG modes with the global and full- $f$  GYSELA code require the equilibrium density function to depend on the motion invariants only. If not, the generated strong mean flows can completely quench turbulent transport.

(Some figures in this article are in colour only in the electronic version)

## 1. Introduction

In strongly magnetized plasmas such as tokamak plasmas, turbulence develops on micro-scales in the transverse direction, typically of the order of a few Larmor radii. However, its non-linear saturation is largely governed by large scale flows, which can capture most of the turbulent energy without driving any transverse transport [1]. Obviously, such a regime is highly desirable in the quest for fusion energy. As such, it deserves much theoretical, numerical

(see [2] and references therein) and experimental [3] attention. Such flows can be generated by the turbulence itself via non-linear coupling, the so-called zonal flows, or by the equilibrium, leading to mean flows. This paper contributes to this effort by means of kinetic and fluid simulations and analytical predictions. The driving mechanism and the impact on turbulence of the large scale flows is explored, including zonal flows, geodesic acoustic modes (GAMs) and mean flows.

In section 2, kinetic and fluid non-linear simulations of the interchange instability are compared, using the same numerical code. The fluid simulations always overestimate the turbulent transport, even when the zonal flows are artificially suppressed. Section 3 details the role of zonal flows in transport barriers characterized by a large density gradient in a drift-kinetic model for slab ion temperature gradient (ITG) turbulence. Finally, if the initial state does not depend on the motion invariants only—that is to say, if it does not correspond to a true stationary equilibrium, large scale stationary flows are shown to develop in a full  $f$  gyrokinetic model for toroidal ITG turbulence, section 4. At later times, the system self-consistently develops a parallel current to counterbalance this vertical charge separation governed by the curvature drift. In this framework, any error in the conservation of the motion invariants results in the generation of equilibrium poloidal flows. Since these flows decay to a non-vanishing magnitude in the collisionless limit, they may prevent the onset of turbulence.

## 2. Reduced 3D simulations: kinetic versus fluid descriptions

The fluid description of turbulent transport in magnetized plasmas requires less numerical resources, both in CPU-time and memory, than the kinetic approach. However, fundamental aspects of plasma physics, namely resonant wave–particle interactions, cannot be properly accounted for by fluid theories. Also, collisional closures of the fluid hierarchy lead to an overdamping of zonal flows [4], which are known to govern the turbulent transport magnitude [1]. As a result, fluid models overestimate both the linear instability threshold and the effective transport coefficients [5]. The present section addresses these issues in a reduced electrostatic model for interchange turbulence. Comparing fluid and kinetic descriptions of the same instability up to the non-linear regime provides a powerful way of testing the efficiency of fluid closures. Using the same simulation code allows one to exclude any discrepancy due to the numerics.

*The model.* Let us consider a magnetized plasma in cylindrical geometry, such that the magnetic field  $B$  is along the angular direction. Assume the perturbations are constant along the field lines—flute assumption, the system is 2D in space, the radial and azimuthal directions. Only periodic solutions in the latter direction are retained. In the limit of large wavelengths as compared with the thermal ion Larmor radius, namely  $k_{\perp}\rho_i \ll 1$ , the drift-kinetic model is further reduced to 1D-in-energy, by only considering  $v_{\parallel} = 0$  ions. In this case, the curvature drift  $v_{B \times \nabla B}$  is proportional to the kinetic energy  $E \propto v_{\perp}^2$ . When restricting the analysis to an annulus of small extension as compared with its mean radius  $R_0$ ,  $\vec{v}_{B \times \nabla B} \equiv E v_d \vec{e}_y$  can be taken constant in space, and the geometry becomes cartesian. Here,  $v_d = \rho_i/R_0$  and  $E$  is normalized to the constant temperature  $T_0$ . In the electrostatic regime, the ions are governed by the following kinetic system:

$$\partial_t f + [\phi, f] + v_d E \partial_y f = 0, \quad (1)$$

$$\phi - \langle \phi \rangle - \nabla_{\perp}^2 \phi = \frac{1}{n_{\text{eq}}} \int_0^{\infty} f \, dE - 1. \quad (2)$$

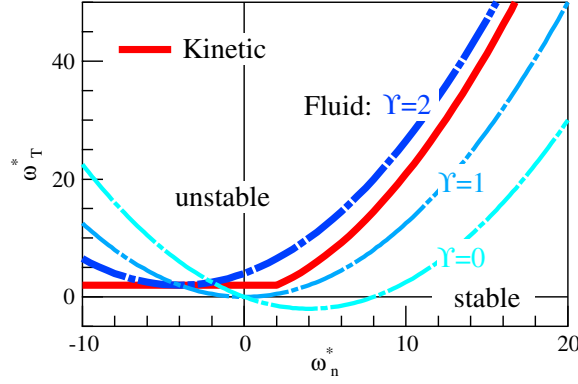


Figure 1. Linear stability diagram of the interchange instability.

Electrons are assumed adiabatic.  $\langle \phi \rangle$  denotes the average over  $y$ . Here,  $x$  and  $y$  refer to the radial and azimuthal coordinates, respectively, normalized to  $\rho_s = \sqrt{mT_0}/eB_0$ .  $T_0$  and  $B_0$  are constant temperature and magnetic field, respectively. The Poisson brackets, accounting for the advection by the  $\vec{E} \times \vec{B}$  drift, are defined by  $[\phi, f] = \partial_x \phi \partial_y f - \partial_y \phi \partial_x f$ . The time is normalized to  $\omega_{ci}^{-1} = m/eB_0$ .

When restricting to the first two fluid moments, namely, density  $n = \int_0^\infty f dE$  and the pressure  $p = \int_0^\infty f E dE$ , the fluid version of the kinetic system equations (1) and (2) reads as follows:

$$\partial_t n + [\phi, n] + v_d \partial_y p = \nabla_\perp \cdot (D \nabla_\perp n), \quad (3)$$

$$\partial_t p + [\phi, p] + v_d \partial_y Q = \nabla_\perp \cdot (D \nabla_\perp p). \quad (4)$$

Here, due to the adiabaticity of the electrons, the density relates to the potential:  $n = n_{\text{eq}}(1 + \phi - \langle \phi \rangle - \nabla_\perp^2 \phi)$ .  $Q \equiv \int f E^2 dE$  represents the heat flux. Simple closures can be envisaged, leading to  $Q \propto pT$ . Various values of the coefficient of proportionality  $\Upsilon$  can be derived. They correspond either to a vanishing flux ( $\Upsilon = 0$ ) or to the vanishing departure of the energy to the temperature  $\int (E - T)^2 f dE = 0$  ( $\Upsilon = 1$ ) or finally to the Maxwellian approximation  $\int (f - f_M) E^2 dE = 0$  ( $\Upsilon = 2$ ), where  $f_M$  is the equilibrium Maxwellian distribution function  $f_M = (n_{\text{eq}}/T_{\text{eq}}) \exp\{-E/T_{\text{eq}}\}$ . These closures do not account for any kinetic effect [6]. Conversely, small scales are damped through the ad hoc diffusive coefficient  $D(x)$ , as will be detailed in the linear analysis. For stability reasons,  $D$  is given a large magnitude in buffer regions close to both radial boundaries. This issue is extensively discussed in [7].

*Linear analysis.* The kinetic system equations (1) and (2) exhibits a linear instability threshold when perturbed around an initial Maxwellian equilibrium  $f_M$ . Introducing the drift frequency  $\omega_d = k_y T_{\text{eq}} v_d$ , the dispersion relationship is as follows:

$$1 + \int_0^\infty d\zeta e^{-\zeta} \frac{\omega_n^* + \omega_T^*(\zeta - 1)}{\omega - \omega_d \zeta} = 0. \quad (5)$$

The corresponding linear stability diagram is plotted in figure 1. For a vanishing equilibrium density gradient, it reads  $\omega_{T, \text{kin}}^*, \text{crit} = (1 + k_\perp^2) \omega_d$ . The diamagnetic frequency is  $\omega_T^* = k_y T_{\text{eq}}/L_T$ ,

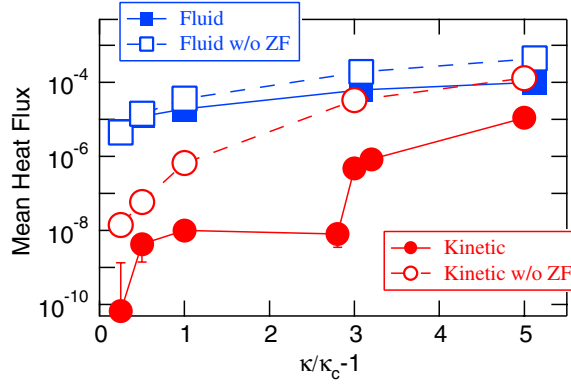


**Figure 2.** Mean turbulent heat flux  $q_T = \langle \tilde{T} \tilde{v}_{Ex} \rangle$  at mid-radius as a function of the departure from the equilibrium, namely  $\omega_T^*/\omega_T^{*,\text{crit}} - 1$ .

with  $L_T$  the temperature gradient length (with the axis convention,  $L_T^{-1} \equiv d \log(T_{\text{eq}})/dx$  is positive). The asymmetry with regard to the vertical axis is governed by the resonance condition equation (5), which imposes  $\omega/\omega_d \geq 0$ . The horizontal branch corresponds to the resonant part. As far as the fluid threshold is concerned, it depends on the closure assumption. Three cases are plotted in figure 1. As expected, they mimic the non-resonant parabolic branch of the kinetic system. Ultimately, the relative discrepancy between fluid and kinetic thresholds vanishes for  $\omega_n^* \rightarrow +\infty$ . For  $\omega_n^* = 0$ , the inviscid fluid threshold is  $\omega_{T,\parallel}^{*,\text{crit}} = \Upsilon(\Upsilon - 1)(1 + k_\perp^2)\omega_d$ .

*Fluid equivalent to  $f$  at two energies.* So as to perform fine comparisons between fluid and kinetic results, and especially to rule out any discrepancy due to the numerics, the same numerical code is used, based on the semi-Lagrangian scheme [8]. In this framework, it is interesting to note that equations (3) and (4) can be recast in a system involving two monokinetic distribution functions  $f_\pm(x, y, t)$ , at the energy  $E_\pm = T_0 \pm \varepsilon$ , respectively. Here,  $\varepsilon$  is a parameter, while density and pressure are defined by  $n \equiv f_+ + f_-$  and  $p \equiv E_+ f_+ + E_- f_-$ . The new system is the following:

$$\partial_t f_\pm + [\phi, f_\pm] + v_d E_\pm \partial_y f_\pm = \nabla_\perp \cdot (D \nabla_\perp f_\pm). \quad (6)$$

Such a system leads to the fluid system equations (3) and (4) with the following closure:  $Q = pT + 4\varepsilon^2 f_+ f_- / n$ . It is equivalent to  $\Upsilon = 1$  in the limit  $\varepsilon = 0$ . At  $\omega_n^* = 0$ , the linear threshold is given by  $\omega_{T,f_\pm}^{*,\text{crit}} = (1 + k_\perp^2)(\varepsilon^2 \omega_d + ((DT_{\text{eq}})^2 k_\perp^4 / \omega_d))$ .

*Non-linear comparison.* The fluid parameters  $D$  and  $\varepsilon$  are chosen so as to lead to similar linear properties as for the kinetic system, namely the same threshold and unstable  $k$ -spectrum. In this case, the maximum fluid growth rate is twice the one of the kinetic simulation. These two cases are then compared in the non-linear regime. Fluctuations are zero at both radial ends, such that the temperature is prescribed at these boundaries. The simulations are performed with an initial linear temperature profile, the density profile being flat. The full symbols in figure 2 show the mean turbulent heat flux  $q_T = \langle \tilde{T} \tilde{v}_{Ex} \rangle$  at the centre of the simulation box, with  $\tilde{v}_{Ex} \equiv -\partial_y \tilde{\phi}$ , as a function of the departure from the linear threshold. This graph is analogous to the one reported in [5], with the additional constraint that all data points are obtained here with the same numerical code. Two main results are evident from the graph. First, whatever the driving term amplitude, fluid simulations always predict larger turbulent

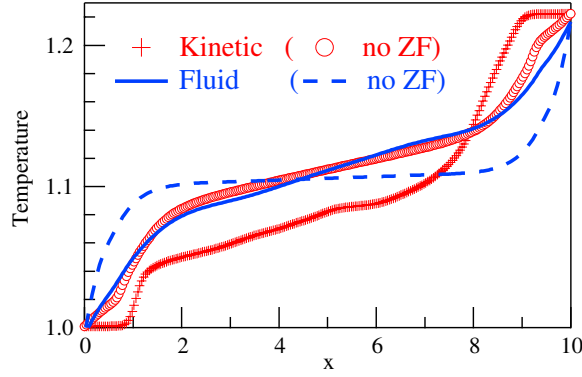
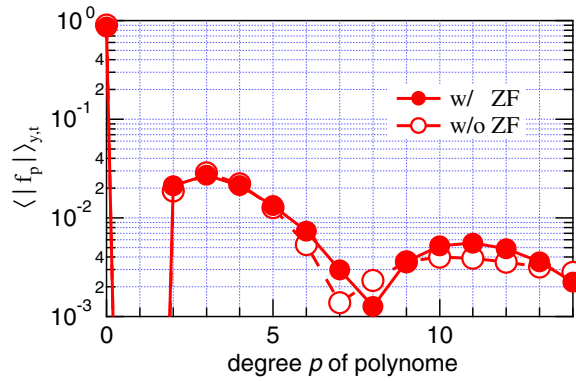


Figure 3. Mean temperature profiles for the four runs at  $\omega_T^*/\omega_T^{*,\text{crit}} \approx 4$  (cf figure 2).

transport than kinetic ones, by orders of magnitudes, although the discrepancy reduces at large forcing. Second, the kinetic transport exhibits a sharp transition at about  $\omega_T^*/\omega_{T,\text{kin}}^{*,\text{crit}} \approx 4$ . This sharp increase is governed by an increase in both the magnitude and the phase shift of the fluctuations. Below this transition point, the turbulent flux is almost vanishing, most of the turbulent energy being captured by the zonal flows. This behaviour is reminiscent of the non-linear threshold observed in [5], sometimes referred to as the Dimits'upshift. Surprisingly, there is no significant variation in the zonal flows magnitude, or in their shearing, at this transition. Conversely, when the transition occurs, the shearing rate  $\omega_E$  governed by the zonal flows becomes of the same order of magnitude as the growth rate of the most unstable mode in the system [9]. Although this does not provide an explanation, such a result looks consistent with formulae predicting turbulence suppression when  $\gamma_{\text{max}}/\omega_E$  becomes of the order of unity [10].

While zonal flows remain undamped in the present collisionless kinetic model, they are linearly damped by the diffusive coefficient in the fluid approach, equation (6). Therefore, they provide a plausible explanation for the observed discrepancy. In this framework, another set of fluid and kinetic simulations has been performed, with zonal modes artificially suppressed. This allows one to discriminate between zonal flow effects and other kinetic peculiarities. These are the open symbols in figure 2. As expected, the turbulent transport increases significantly, by orders of magnitudes in kinetics and factors in fluids. Also, the kinetic turbulent flux increases smoothly, without any sharp transition in this case. It is worth noting that, for a given transport magnitude, kinetic and fluid simulations lead to similar temperature profiles, figure 3. However, there is still some discrepancy between the magnitude of the transport in kinetic and fluid simulations—although reduced as compared with the case with zonal flows, the latter still overestimating the turbulence. Therefore, the mismatch between kinetic and fluid predictions cannot be attributed to the sole zonal flow dynamics.

Projecting the distribution function onto the ortho-normal basis of the Laguerre polynomials  $L_p(\zeta)$  allows one to quantify its departure from the maxwellian:  $f(x, y, E, t) = \sum_{p=0}^{\infty} \hat{f}_p(x, y, t) L_p(\zeta) e^{-\zeta}$ , with  $\hat{f}_p \equiv \int_0^{\infty} L_p f d\zeta$ . The number of fluid moments required to properly account for the deformation of the distribution function in the non-linear regime can then be estimated. Indeed, any fluid moment of order  $k$  is uniquely decomposed into the polynomials  $L_{p \leq k}$  [7]. The coefficients  $\hat{f}_p$ , plotted in figure 4, are only slowly decaying towards zero. Consequently, a large number of fluid moments would be required, unless an appropriate closure succeeds in accounting for these high order moments. Since this slow



**Figure 4.** Coefficients of the projection onto Laguerre polynomials of the distribution function in the turbulent regime. Open symbols refer to a run without zonal flows.

decay is also observed in the absence of zonal flows, this can explain why kinetic and fluid results still differ in this regime.

### 3. Role of zonal flows in transport barriers

Tokamak plasmas can spontaneously bifurcate towards highly confined regimes, characterized by radially localized regions with weak turbulent transport [12]. According to standard theories, these transport barriers develop when the poloidal velocity shear is sufficiently large [10] or when the magnetic shear is either negative or vanishing [13, 14]. The role of density gradient is investigated non-linearly in the 4D version of the GYSELA code [8], describing the slab branch of ITG turbulence [11]. As reported in [15], the temperature profile tends to relax when the initial density profile is flat, leading to a low confinement regime. Conversely, a transport barrier can spontaneously develop for a peaked initial density profile. It is well known that a large density gradient is linearly stabilizing for slab ITG modes. However this is not the main ingredient here. Indeed zonal flows appear to play a crucial role. The difference in behaviour between peaked and flat density profiles can be understood by analysing the mechanism of turbulent flow generation in the presence of a density gradient. The driving source of zonal flows, namely the Reynolds stress, is found to depend sensitively on the density gradient. Indeed, a quasi-linear analysis shows that a small density gradient length leads to large values of the stress tensor. Such a process might help in understanding those barriers characterized by large density gradients [16].

Last but not least, the barrier is found to locate at an extremum of flow curvature, rather than at flow shear as usually reported. This property is recovered by analysing the stability in the presence of a slowly varying shear flow. The radial structure of a mode obeys a Schrödinger-like equation, the effective potential depending on the flow curvature. Perturbative theory shows that, when the curvature of zonal flows is located at the maximum of the temperature gradient and is large enough, the potential exhibits an anti-well structure that expels the modes from this region. The gradient can then steepen and possibly lead to a transport barrier. Understanding the saturation mechanism of such a process, and especially predicting the width of the barrier, remains a challenging issue. Finally, the Kelvin–Helmoltz instability cannot be advocated in the dynamics. Indeed, the fluctuations die away when the system is forced with similar poloidal flows to those observed in the non-linear runs, but vanishing diamagnetic frequencies.

#### 4. Global full- $f$ simulations of toroidal ITG turbulence

There is a rich variety of 5D gyrokinetic codes to tackle the problem of core turbulent transport in weakly collisional tokamak plasmas. They are either global, allowing for the physics of large scale events, or local using flux tube geometry allowing for small scale structure studies. The numerical scheme is either Eulerian [17], known to be dissipative, or Lagrangian such as in particle-in-cell codes [1, 18]. The latter suffer from noise [19] that can be minimized by optimized loading techniques [20]. Only the departure from the equilibrium  $\delta f$  is usually modelled for this reason. In the GYSELA code, the full distribution function is evolved in the global geometry, using the semi-Lagrangian scheme with moderate dissipation and weak noise. With such a full- $f$  model, where no scale separation is assumed, flux driven systems can be studied [21].

The GYSELA code models toroidal ITG turbulence in 5D. Using the normalization of previous sections, the ion distribution function obeys the following system:

$$\partial_t f + (\vec{v}_E + \vec{v}_g) \cdot \vec{\nabla}_\perp f + v_\parallel \nabla_\parallel f + v_\parallel \partial_{v_\parallel} f = 0, \quad (7)$$

$$\frac{1}{T_e} (\phi - \langle \phi \rangle) - \frac{1}{n_0} \vec{\nabla}_\perp \cdot (n_0 \vec{\nabla}_\perp \phi) = \frac{1}{n_0} \int d\Gamma J \cdot (f - f_{\text{eq}}), \quad (8)$$

with  $\vec{v}_E = (\vec{b}/B) \times \vec{\nabla} J \cdot \phi$ ,  $\vec{v}_g = (v_\parallel^2/B + \mu) \vec{b} \times (\vec{\nabla} B/B)$  and  $v_\parallel = -\nabla_\parallel (J \cdot \phi) - \mu \nabla_\parallel B + v_\parallel \vec{v}_E \cdot (\vec{\nabla} B/B)$ .

The gyro-average operator  $J$  is approximated by a second order Padé fraction [7]. The phase-space volume element is  $d\Gamma \equiv B d\mu dv_\parallel$ , and  $\nabla_\parallel = (1/R_0)(\partial_\phi + (1/q)\partial_\theta)$ . The magnetic equilibrium is circular, with  $B = R_0/R$  and  $\vec{b} = |\vec{b}|^{-1}(\hat{e}_\phi + (r/qR_0)\hat{e}_\theta)$ . Three parameters govern the safety factor:  $q = q_0 + \delta_q (r/a)^{\alpha_q}$ . The normalized equilibrium distribution function is  $f_{\text{eq}} = n_{\text{eq}}/(\sqrt{2\pi} T_{\text{eq}}^{3/2}) \exp\{-(v_\parallel^2/2 + \mu B)/T_{\text{eq}}\}$ .

Choosing  $f_{\text{eq}}$  as function of the motion invariants is crucial for these full- $f$  simulations. Breaking this rule leads to the development of large scale steady flows, which prevent the onset of turbulence, consistently with previous observations [22, 23]. In particular, the equilibrium profiles  $n_{\text{eq}}$  and  $T_{\text{eq}}$  cannot depend on the magnetic flux  $\psi$  only. Conversely, one can construct an effective normalized radius  $\bar{r}$  out of the normalized canonical toroidal momentum  $P_\varphi \equiv \psi + Rv_\varphi$ . One possible and convenient choice, which only depends on the three motion invariants of the system, namely the energy, the toroidal momentum and the adiabatic invariant, is  $\bar{r} = r_p - (q_p/r_p)\{\tilde{\psi}(r) - \tilde{\psi}(r_p) - (Rv_\parallel - R_0\bar{v}_\parallel)\}$ . The subscript  $p$  refers to the centre of the radial box, and  $\tilde{\psi} \equiv -\int_0^r (r dr/q)$ . Finally,  $\bar{v}_\parallel = \text{sign}(v_\parallel)vH(v)$ , with  $v \equiv \{2(E - \mu B_{\text{max}})\}^{1/2}$  and the Heaviside function  $H$  aims at subtracting the mean parallel velocity of the passing ions only. Such a definition has the advantage of minimizing the difference between  $\bar{r}$  and the geometrical radius  $r$ . Interestingly, introducing  $\bar{r}$  makes  $f_{\text{eq}}$  asymmetric in  $v_\parallel$ . The resulting parallel ion flow counter-balances the vertical charge separation due to the curvature drift  $\vec{v}_g$ . It is analogous to the Pfirsch–Schlüter current. In the absence of electric field, any solution of equations (7) and (8) exhibits such a mean parallel flow [24]. Numerical simulations show that such a parallel current self-consistently develops when starting from an initial distribution function symmetric in  $v_\parallel$ . It follows the build-up of an essentially up–down electric potential, which is governed by the vertical charge separation. In addition, any default in the conservation of the motion invariants leads to the generation of spurious equilibrium flows, i.e.  $(m, n) = (0, 0)$ . Such mean flows do not vanish towards zero, as predicted theoretically [4]. Conversely, the initial

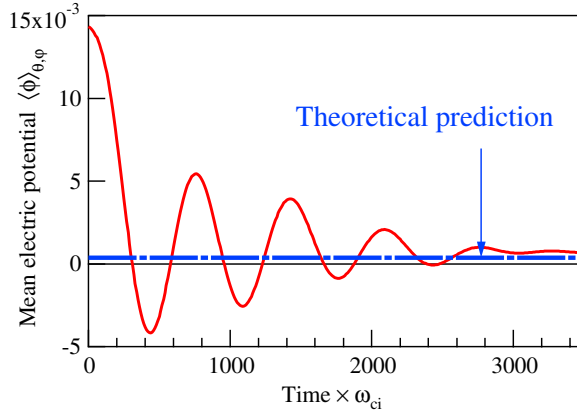


**Figure 5.** The initial  $(m, n) = (0, 0)$  flow decays towards the predicted theoretical value with the GAM frequency.

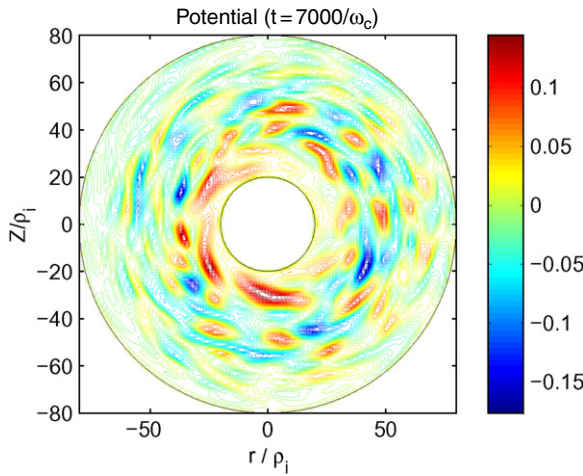


**Figure 6.** Typical poloidal cross-section of the electric potential in the turbulent regime. The time averaged  $(m, n) = (0, 0)$  component has been subtracted.

flow magnitude is shielded by finite orbit width effects, so that the flow decays towards the non-vanishing theoretical value, namely  $\langle v_\theta \rangle_\infty = \langle v_\theta \rangle_0 (1 + 1.6q^2/\epsilon^{1/2})^{-1}$ , as exemplified in figure 5. As expected, this decay exhibits transitory oscillations at the GAM frequency  $\omega_{\text{GAM}} = \{7/2 + T_e + T_i\}^{1/2}/R$ .

In this framework, and since large magnitude mean flows can prevent the onset of turbulence, it is critical for full- $f$  codes to ensure good conservation properties of the motion invariants, so as to avoid any source of spurious  $\langle v_\theta \rangle$ . The good conservation properties of the adopted numerical scheme allows for the development of turbulence. Figure 6 shows a snapshot of the electric potential in the turbulent regime. It exhibits the characteristic ballooning shape in the low field side, while the typical structure size is of the order of a few ion Larmor radii.

## 5. Conclusion

Large scale flows are known to strongly govern turbulence and transport in the kinetic regime. They may be generated by the turbulence itself, the zonal flows, or by the equilibrium, leading to mean flows. The case of zonal flows is examined in detail. Strong density gradients are found to favour their excitation by increasing the magnitude of the Reynolds stress. Conversely to standard theories, the curvature of zonal flows is here the key stabilizing parameter, possibly by repelling the unstable modes from the regions of maximum temperature gradient. Such a process can even lead to transport barriers. Since zonal flows are overdamped in fluid simulations, they provide a plausible explanation for the larger turbulent transport as compared with kinetic predictions. Using the same numerical tool for both descriptions of the interchange instability, we show however that zonal flows cannot account for the whole discrepancy. The large number of fluid moments required to describe the kinetic results is advocated. Finally, strong mean flows are observed when the equilibrium distribution function does not depend on the motion invariants only or when these are not properly conserved. In this framework, the good conservation properties of the full- $f$  gyrokinetic code GYSELA is highly beneficial.

## Acknowledgments

We wish to acknowledge the strong commitment of C Passeron and R David in the numerical development of the code. Fruitful discussions with M Ottaviani and A Smolyakov on fluid closures are also acknowledged.

## References

- [1] Lin Z, Hahm T S, Lee W W, Tang W M and Diamond P H 1999 *Phys. Rev. Lett.* **83** 3645
- [2] Diamond P H, Itoh S-I, Itoh K and Hahm T S 2005 *Plasma Phys. Control. Fusion* **47** R35–161
- [3] Fujisawa A *et al* 2004 *Phys. Rev. Lett.* **93** 165002  
Coda S, Porkolab M and Burrell K 2001 *Phys. Rev. Lett.* **86** 4835  
Moyer R *et al* 2001 *Phys. Rev. Lett.* **87** 135001  
Shats M and Solomon W 2002 *Phys. Rev. Lett.* **88** 045001  
Jakubowski M, Fonck R and McKee G 2002 *Phys. Rev. Lett.* **89** 265003
- [4] Rosenbluth M N and Hinton F L 1998 *Phys. Rev. Lett.* **80** 724
- [5] Dimits A M *et al* 2000 *Phys. Plasmas* **7** 969
- [6] Hammett G W and Perkins F W, 1990 *Phys. Rev. Lett.* **64** 25
- [7] Sarazin Y *et al* 2005 *Plasma Phys. Control. Fusion* **47** 1817
- [8] Grandgirard V *et al* 2006 *J. Comput. Phys.* **217** 395–423
- [9] Fleurence E 2005 Descriptions fluide et cinétique d'une turbulence d'interchange dans un plasma magnétisé  
*PhD Thesis* Université Henri Poincaré, Nancy-I (France)
- [10] Biglari H, Diamond P H and Terry P 1990 *Phys. Fluids B* **2** 1  
Hahm T S and Burrell K H 1995 *Phys. Plasmas* **2** 1648  
Waltz R E *et al* 1995 *Phys. Plasmas* **2** 2408
- [11] Coppi B, Rosenbluth M N and Sagdeev R Z 1967 *Phys. Fluids* **10** 582
- [12] Wagner F *et al* 1982 *Phys. Rev. Lett.* **49** 1408  
Wolf R C 2003 *Plasma Phys. Control. Fusion* **45** R1–91
- [13] Diamond P H *et al* 1997 *Phys. Rev. Lett.* **78** 1472  
Newman D *et al* 1998 *Phys. Plasmas* **5** 938
- [14] Garbet X *et al* 2001 *Phys. Plasmas* **8** 2793
- [15] Sarazin Y *et al* 2006 *Phys. Plasmas* **13** 092307
- [16] Mertens V *et al* 1990 *Plasma Phys. Control. Fusion* **32** 965–81
- [17] Dorland W, Jenko F, Kotschenreuther M and Rogers B N 2000 *Phys. Rev. Lett.* **85** 5579  
Jenko F 2000 *Comput. Phys. Comm.* **125** 196  
Candy J and Waltz R E 2003 *J. Comput. Phys.* **186** 545

- 
- [18] Idomura Y, Tokuda S and Kishimoto Y 2003 *Nucl. Fusion* **43** 234–43  
Villard L *et al* 2004 *Nucl. Fusion* **44** 172
- [19] Nevins W M *et al* 2005 *Phys. Plasmas* **12** 122305
- [20] Hatzky R *et al* 2002 *Phys. Plasmas* **9** 898
- [21] Darmet G *et al* 2008 Intermittency in flux driven kinetic simulations of trapped ion turbulence *Comm. Nonlin. Sci. Numer. Simul.* **13** at press
- [22] Idomura Y, Tokuda S and Kishimoto Y 2003 *Nucl. Fusion* **43** 234
- [23] Angelino P *et al* 2006 *Phys. Plasmas* **13** 052304
- [24] Dif-Pradalier G *et al* 2008 Defining an equilibrium state in global full- $f$  gyrokinetic models *Comm. Nonlin. Sci. Numer. Simul.* **13** at press